

SpecFLASH: A Latent-Guided Semi-autoregressive Speculative Decoding Framework for Efficient Multimodal Generation

Zihua Wang ^{*1} Ruibo Li ^{*2} Haozhe Du ^{*1} Joey Tianyi Zhou ³ Yu Zhang ¹ Xu Yang ¹

Abstract

Large language models and large multimodal models (LLMs and LMMs) deliver strong generative performance but suffer from slow decoding, a problem that becomes more severe when handling visual inputs, whose sequences typically contain many more tokens with lower information density than text. Speculative decoding accelerates LLM inference by letting a compact draft model propose candidate tokens that are selectively accepted by a larger target model, achieving speed-up without degrading quality. However, existing multimodal speculative decoding approaches largely ignore the structural characteristics of visual representations and usually rely on text-only draft models. In this paper, we introduce SpecFLASH, a speculative decoding framework tailored to LMMs that explicitly exploits multimodal structure when designing the draft model. We first mitigate redundancy in visual token sequences with a lightweight, latent-guided token compression module that compacts visual features while preserving semantics, and then leverage the co-occurrence and local correlations of visual entities via a semi-autoregressive decoding scheme that predicts multiple tokens in a single forward pass. Extensive experiments demonstrate that SpecFLASH consistently surpasses prior speculative decoding baselines, achieving up to $2.68\times$ speed-up on video captioning and $2.55\times$ on visual instruction tuning, relative to the original LMM. Our code is available [\[here\]](#).

1. Introduction

Large multimodal models (LMMs) (Achiam et al., 2023; Team et al., 2024; Yang et al., 2024; Liu et al., 2023) have

^{*}Equal contribution ¹Southeast University, Nanjing, China
²Nanyang Technological University, Singapore ³A*STAR Centre for Frontier AI Research (CFAR), Singapore. Correspondence to: Xu Yang <xuyang.palm@seu.edu.cn>.

Under review.

made significant progress on tasks like video captioning and visual question answering by leveraging synergistic relationships between data types. Recent studies show that processing more input tokens during inference improves contextual understanding (Muennighoff et al., 2025; Liu et al., 2025). As a result, LMMs increasingly adopt finer-grained patch division strategies, which significantly expand the token count. This issue is particularly severe for video inputs, as the large number of the video frames leads to a significant expansion of the visual input scale. While larger models and longer contexts improve accuracy and flexibility, they also raise deployment challenges due to hardware constraints and increased computational costs.

To address the efficiency issue, recent works propose token compression to remove some visual tokens (Zhang et al., 2025; Wen et al., 2025). Since the visual tokens contain superfluous or non-essential information, pruning these tokens makes shorter input contexts and thus accelerating the generation. However, this simplification comes with potential drawbacks. For example, it can be difficult to accurately identify which tokens to prune, as seemingly non-critical tokens may actually encode latent task-specific cues (Wen et al., 2025). Therefore, while token compression offers efficiency gains, it may damage the performance by oversimplifying the visual input, especially in fine-grained multimodal tasks.

Speculative decoding offers a promising solution for accelerating inference without sacrificing performance. As an effective strategy for speeding up decoding in Large Language Models (LLMs) (Bachmann et al., 2025; Li et al., 2024b; Cai et al., 2024; Fu et al., 2024), it employs a lightweight draft model to quickly generate candidate token sequences, which are then verified in parallel by the target model through a **single forward pass**. Crucially, by applying specific acceptance-rejection criteria, the accepted tokens can be regarded as samples from the target model’s distribution, thereby preserving output quality. This fail-safe property ensures that speculative decoding maintains the accuracy of the target model while significantly reducing inference latency. However, the overall speed-up is closely linked to the acceptance rate of the candidates generated by the draft model. This relationship establishes a critical trade-off in the design of draft models: overly simplistic architectures,

while computationally efficient, risk producing low-quality candidates that are frequently rejected during verification, diminishing overall latency gains.

Given that LMMs frequently leverage LLMs as their decoders, prior work (Gagrani et al., 2024) has attempted to directly transplant speculative decoding techniques from LLMs to the multimodal settings. However, this method trains a separate draft model using *only textual inputs*, which introduces additional computational overhead and ignores the visual modality. To overcome this drawback, early efforts (Ganesan et al., 2025; Hu et al., 2025) have explored incorporating both visual and textual information into the draft model. However, in contrast to LLMs, LMMs contain numerous redundant visual tokens, making a naive extension of this framework to multimodal input computationally expensive. To address this limitation, we propose SpecFLASH (Speculative Decoding with Fast Latent-Aware Semi-autoregressive Heuristics), a novel method for efficient multimodal speculative decoding that achieves a favorable trade-off between inference speed and draft quality.

In this work, we leverage two distinctive properties of multimodal data to enhance the efficiency of SpecFLASH: visual token redundancy and vision object co-occurrence. Based on these properties, we design two novel components in the draft model: visual token compression and semi-autoregressive head. Unlike LLMs, LMMs often process a large number of redundant visual tokens, which significantly slow down inference during speculative decoding. To mitigate this, we compress the visual tokens based on the hidden state features, which accelerates draft generation while minimizing the loss of semantic information. Speculative decoding speeds up autoregressive generation using a lightweight draft model to predict the output of a heavier target model. However, since the draft model remains autoregressive, the overall speed-up is limited. We observe that although relational phrases (e.g., “on the table” and “in front of”) are not unique to LMMs, they become substantially more constrained and deterministic when conditioned on an image. In text-only generation, such relations are determined purely by discourse intent and can vary widely given the same prefix. In contrast, in vision–language generation, once the model identifies salient objects and their spatial configuration (e.g., a cup on a table), the corresponding relational description strongly co-occurs and is far more predictable. This observation motivates our adoption of a semi-autoregressive decoding strategy, which better preserves spatial relationships while maintaining generation efficiency.

By combining latent-aware visual token compression with semi-autoregressive decoding, SpecFLASH achieves faster inference and maintains high draft quality. We evaluate SpecFLASH on video captioning and visual instruc-

tion tuning tasks, using LLaVA (Shang et al., 2024) and QwenVL (Bai et al., 2025) as target models. Experimental results demonstrate that the two components of SpecFLASH, visual token compression and semi-autoregressive decoding, provide distinct yet synergistic advantages on different tasks. In video captioning, where a large number of visual tokens are involved, visual token compression is particularly effective, while in instruction tuning, which typically involves fewer visual tokens but longer textual inputs, the semi-autoregressive decoding contributes more significantly to efficiency gains. Overall, SpecFLASH achieves average speed-up gains of 24.4% and 41.5% on video captioning and visual instruction tuning tasks, compared to the previous methods that rely solely on text tokens.

We make the following contributions:

- (1) We propose SpecFLASH, a novel speculative decoding framework for LMMs that effectively exploits the characteristics of multimodal inputs.
- (2) By observing that visual information is often redundant and descriptions of visual content typically appear as short phrases, we introduce visual token compression and semi-autoregressive generation to accelerate draft inference.
- (3) Experiments show that SpecFLASH achieves substantial acceleration without degradation in output quality.

2. Related Works

Speculative decoding. Since the introduction of speculative sampling (Leviathan et al., 2023; Chen et al., 2023), the strategy of using light-weight models to generate drafts, with large models performing parallel verification, has been widely adopted to accelerate inference across various LLMs (Xia et al., 2024b; Gao et al., 2025). However, selecting an appropriate draft model is challenging, as it is difficult to make the predicted distribution consistent with that of the target model due to differences in model size or architecture (Bachmann et al., 2025). It has been suggested that knowledge distillation applied to the target model can produce a compact model with a higher reception rate (Zhou et al., 2023). Unlike training a draft model independently, self-speculative decoding introduces a way to reuse components of the target model (Liu et al., 2024a; Elhoushi et al., 2024; Xia et al., 2024a). Following this idea, Eagle (Li et al., 2024b;c) introduces an autoregressive head on the second-to-top feature extracted by the target model to predict candidate tokens. Beyond increasing the acceptance rate of draft tokens, enhancing the drafting efficiency further contributes to achieving a higher speed-up ratio in speculative decoding. Medusa applies n-head architecture, where each head predicts one corresponding token (Cai et al., 2024). Look-ahead Decoding leverages an n-gram pool generated through Jacobi iterations, enabling the model to accept multi-token prefixes (Fu et al., 2024). Speculative decoding has also

been extended beyond LLMs to LMMs (Ganesan et al., 2025; Hu et al., 2025; Wang et al., 2025). MASSV (Ganesan et al., 2025) adapts speculative decoding to multimodal settings via self-distillation, and Dream (Hu et al., 2025) enhances draft quality through a specialized cross-attention mechanism on visual and textual features. Despite these advances, applying speculative decoding to LMMs introduces a fundamental challenge: how to effectively integrate both visual and textual modalities while preserving efficiency and accuracy during inference.

Token Compression. Prior studies have shown that incorporating additional inputs can help correct erroneous outputs and enhance model performance (Liu et al., 2025). However, as Large Multimodal Models (LMMs) continue to scale, improving inference efficiency has become increasingly important (Liu et al., 2023; 2024b; Team et al., 2024). A key challenge lies in the high computational cost caused by the large number of visual tokens. To address this, reducing the number of input tokens without sacrificing essential information is considered a crucial strategy. To reduce redundancy, visual tokens can be merged based on their similarity (Shang et al., 2024; Li et al., 2024a). Image token reduction can also be achieved through a Q-Former (Li et al., 2023) to extract visual concepts (Yang et al., 2024; Chen et al., 2024b). However, evidence from recent research indicates that Q-Former leads to some degree of visual information loss (Yao et al., 2024; Fan et al., 2024). Based on the observation that early-layer visual tokens contain more critical information, LLaVA-mini integrates visual features into text tokens through pre-fusion before these layers (Zhang et al., 2025). DART prioritizes the removal of duplicate tokens over the selection of important tokens (Wen et al., 2025).

3. SpecFLASH

3.1. Preliminaries

In this paper, Large Multimodal Model (LMM) processes two data modalities, images and texts. As shown in Figure 1, the image is encoded by a vision encoder and projected into visual embeddings $V = \{V_1, V_2, \dots, V_N\}$, while the text is encoded into textual embeddings $E = \{E_{N+1}, E_{N+2}, \dots, E_M\}$, where N denotes the number of visual tokens, and M represents the total number of input tokens, encompassing both visual and textual components. Subsequently, these embeddings are concatenated and processed through Transformer layers to produce the second-to-top-layer feature $F = \{F_1, F_2, \dots, F_M\}$. Finally, an LM head maps the last feature F_M to a probability distribution over the output vocabulary space, from which the next token T_0 is sampled.

In speculative decoding, the LMM acts as the target model for output validation, while a lightweight draft model pro-

poses K candidate tokens T'_1, \dots, T'_K . During validation, the target model computes the probabilities of these K candidate tokens in parallel within a single forward pass. The acceptance probability of each candidate token is defined as the ratio of its probability under the target model to its probability under the draft model. Subsequently, the tokens are evaluated after obtaining the acceptance probability of each candidate token. For the i -th token T'_i , if accepted, it is retained as part of the output. If rejected, the token and all subsequent candidate tokens, T'_i to T'_K are discarded, the output token at position i is sampled from the residual distribution constructed from the target and draft probabilities (Leviathan et al., 2023).

Given the single-step inference time \mathcal{M}_T and \mathcal{M}_D for the target and draft model respectively, draft model's inference time \mathcal{M}_D is much less than that of the target model \mathcal{M}_T , due to the lightweight architecture of the draft model. Additionally, the verification of K candidate tokens by the target model is performed in parallel, so the time required to verify all K tokens can be approximated by the single-step time \mathcal{M}_T . For speculative decoding, the total time includes the autoregressive draft model generating K tokens and the subsequent verification by the target model, which can be expressed as:

$$\mathcal{M}_T + K \cdot \mathcal{M}_D. \quad (1)$$

When generating i tokens, i.e., the first i tokens of the K candidate tokens are accepted, speculative decoding takes time of $\mathcal{M}_T + K \cdot \mathcal{M}_D$, while standard vanilla autoregressive decoding takes time of $i \cdot \mathcal{M}_T$, since the latter generates i tokens by performing the forward pass i times with the target model. Therefore, the speed-up ratio of autoregressive speculative decoding can be calculated as:

$$\mathcal{R}_{SD} = \frac{i \cdot \mathcal{M}_T}{(\mathcal{M}_T + K \cdot \mathcal{M}_D)}. \quad (2)$$

When the target model is selected, \mathcal{M}_T remains constant. Therefore, to improve the speed-up ratio, it is crucial to reduce the draft generation time $K \cdot \mathcal{M}_D$, while maintaining a high draft quality to ensure a large value of i . To achieve this, we propose a novel method named SpecFLASH, which effectively balances inference speed and draft quality by leveraging the characteristics of multimodal inputs. Following the previous LLM speculative decoding method Eagle (Li et al., 2024b), we construct the textual input \hat{F}_T by concatenating the second-to-top layer textual feature F_T and the token embeddings E . For the visual modality, SpecFLASH introduces a visual token compression module that reduces computational overhead while preserving key visual semantics. To further accelerate decoding, SpecFLASH incorporates a semi-autoregressive head that predicts the next K tokens in parallel, significantly reducing the draft generation time from $K \cdot \mathcal{M}_D$ to approximately \mathcal{M}_D .

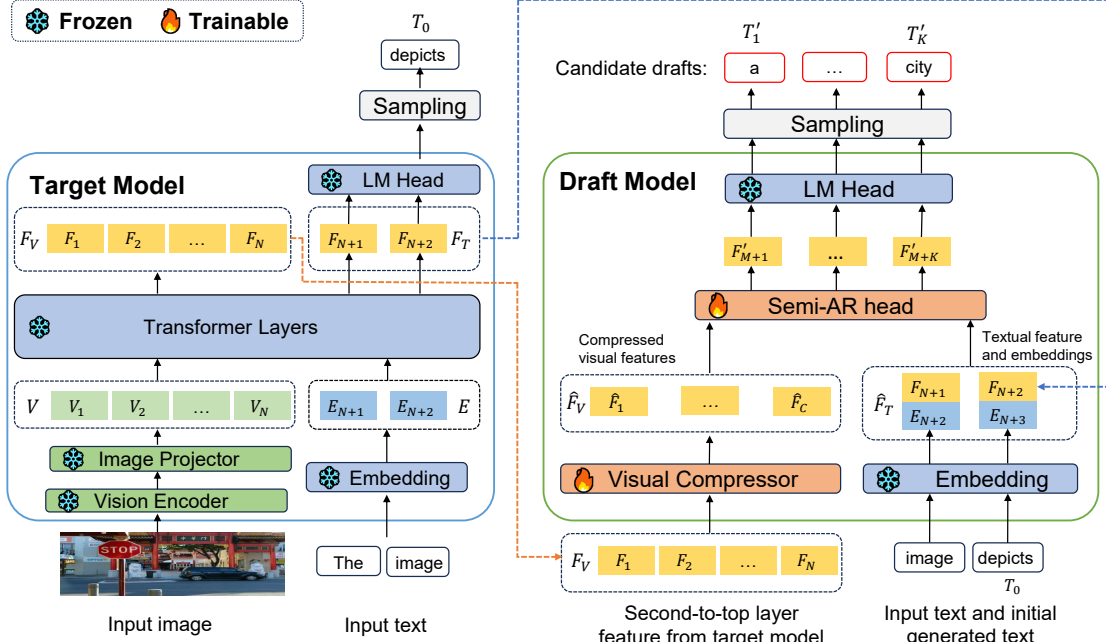


Figure 1. Illustration of SpecFLASH. The target model is depicted on the left, while the draft model is shown on the right. In this example, the number of the total input tokens M is equal to $N + 2$, as the input includes N visual tokens and 2 textual tokens. The draft model takes the second-to-top layer features F_V as the visual input. These features are first compressed by a visual compressor, producing the compressed visual features \hat{F}_V . Along with textual feature and embeddings \hat{F}_T , they are fed into a semi-autoregressive head to generate the next K tokens in parallel. These candidate drafts are highlighted with red-bordered boxes.

3.2. Visual token compression

Unlike LLM speculative decoding methods, our input consists of both visual and textual tokens. Compared to textual tokens, visual tokens are often numerous, leading to a significant increase in inference time (Zhang et al., 2025). To balance the acceleration of draft generation and the potential degradation on acceptance rate, we propose an effective strategy for compressing the visual tokens in the draft model, allowing for faster inference without significantly compromising prediction quality. Since some visual tokens contain redundant information and do not significantly contribute to the final prediction, our goal is to compress the N visual tokens into a smaller set of size C . Specifically, the N -sized visual feature F_V , corresponding to the N visual tokens, is fed into a visual compressor to produce a compressed feature \hat{F}_V of size C . Inspired by the attention mechanism, we introduce a learnable query set \mathcal{C} of size C , where each query is designed to extract information from the feature F_V . By learning a compressed feature representation of size C , the model is able to retain the most salient semantics from the original visual feature. Specifically, the compressed feature \hat{F}_V is computed as:

$$\hat{F}_V = \text{softmax}(\mathcal{C} \cdot F_V^T) \cdot F_V, \quad (3)$$

where \mathcal{C} serves as the query, and visual feature F_V acts as both the key and value in the attention computation. The softmax operation normalizes the attention scores, which

are then used to aggregate F_V into the compressed representation. Eventually, the scale of the visual inputs for the draft model is reduced from N to C .

3.3. Semi-autoregressive inference

In contrast to the previous speculative decoding methods, we introduce a semi-autoregressive head to predict the next K tokens in parallel. Specifically, when generating K candidate tokens, unlike an autoregressive draft model with a runtime of $K \cdot \mathcal{M}_D$ time for performing K inference steps, our semi-autoregressive approach needs only a single inference pass of the draft model, with a runtime of approximately \mathcal{M}_D .

To enable parallel draft decoding, we input K placeholder tokens to denote the future positions without exposing future target tokens. During verification, we apply the standard token-wise acceptance–rejection rule using the draft probabilities produced for each position and the target probabilities computed in parallel by the target model (Leviathan et al., 2023). As Figure 2 shows, the semi-autoregressive head outputs hidden states $F'_{M+1:M+K}$, which are projected by the frozen LM head into probability distributions $P'_{1:K}$, from which candidate tokens $T'_{1:K}$ are sampled.

Our loss function comprises two components. The first is a regression loss, where we employ the Smooth L1 loss to quantify the difference between the features predicted by the

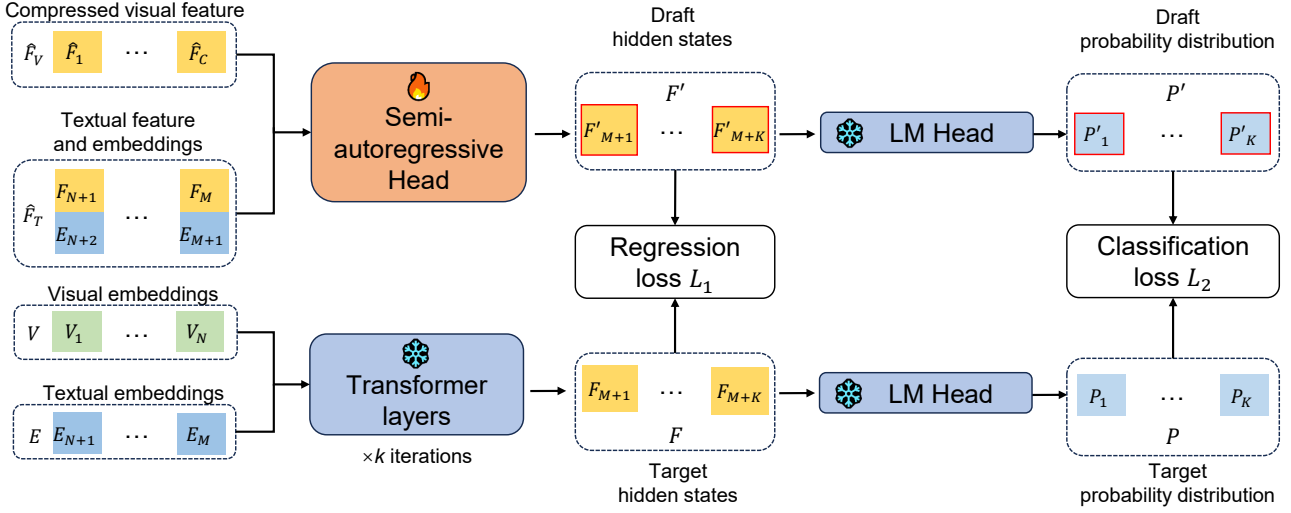


Figure 2. Training procedure with the semi-autoregressive head. The semi-autoregressive head concatenates the compressed visual features \hat{F}_V and the textual features and embeddings \hat{F}_T as input, and subsequently generates the hidden state features F' for the next K tokens. The corresponding probability P for these K candidate tokens are calculated by the frozen LM head from the target model. The semi-autoregressive head is trained using a regression loss, where the feature F from the frozen target model is served as the ground truth, as well as a classification loss, where the draft probability distribution P' is supervised by the output distribution of the target model P .

draft model $F'_{M+1:M+K}$ and those from the target model $F_{M+1:M+K}$. The second component is a classification loss, where we employ the cross-entropy loss to encourage the draft model to generate tokens that align with those produced by the target model. The total loss is defined as:

$$L = \sum_{i=M+1}^{M+K} \ell_{\text{reg}}(F'_i, F_i) + \alpha \cdot \sum_{i=1}^K \ell_{\text{cls}}(P'_i, P_i), \quad (4)$$

where $\ell_{\text{reg}}(\cdot, \cdot)$ and $\ell_{\text{cls}}(\cdot, \cdot)$ denotes the Smooth L1 loss and the cross-entropy loss, respectively. α is a hyper-parameter used to balance the regression and classification losses, ensuring they are of comparable magnitudes. Specifically, α is set to 0.1. After computing the loss at each step, the next token predicted by the target model is appended to the input sequence. The extended sequence is then used to predict the subsequent K tokens. This iterative procedure continues until the entire output sequence is generated.

During inference, the draft model produces K candidate tokens in a single forward pass. These candidate tokens are then sequentially verified by the target model. The draft generation process is outlined in Algorithm 1.

4. Experiments

4.1. Implementation settings

We conduct experiments using LLaVA-1.5 and QwenVL-2.5 as target models. We train and evaluate on video captioning (VC) and visual instruction tuning (VIT), using Kinetics-400 (Kay et al., 2017) and LLaVA-instruct-150k (Liu et al.,

2023), respectively. We use Kinetics-400 mainly as an efficiency stress test with long visual contexts. Since our goal is to accelerate target LMM without changing its output distribution, we use target-generated captions to train the draft model to match the target behavior under the same prompts. For both tasks, we sample 10k instances from each dataset for training. The maximum sequence lengths of training data are set to 200 for VC and 2048 for VIT.

The learning rate is set to 2×10^{-5} and the batch size is set to 8 in our main results. All inferences are performed on a single NVIDIA A6000 GPU with batch size set to 1, following standard practice in prior LLM speculative decoding methods (Li et al., 2024b; Chen et al., 2024c).

We introduce two metrics to evaluate the effectiveness of the speculative decoding: the average acceptance tokens \mathcal{A} and the speed-up ratio \mathcal{R} . The average acceptance tokens \mathcal{A} is defined as the average number of the accepted tokens during a single forward pass of the draft model. Since multiple candidate tokens are generated in parallel during semi-autoregressive inference, the average acceptance tokens \mathcal{A} can be greater than 1, distinguishing it from autoregressive speculative decoding methods. The speed-up ratio \mathcal{R} is adopted as the primary metric to assess the overall efficiency, defined as the generation time of the target model divided by the total time required for speculative decoding including the draft token generation and verification.

4.2. Results

We perform experiments on two typical multimodal tasks: video captioning, which involves a large number of visual to-

Table 1. Quantitative experiments of **video captioning** on LLaVA-1.5 and QwenVL-2.5. We report the results of speed-up ratio \mathcal{R} and the average acceptance tokens \mathcal{A} under temperature $\tau = 0$ and $\tau = 1$. Additionally, we include the average computational cost (FLOPs), for a single round of draft generation and validation. SpecFLASH combines “VisComp” and “SemiAR”, achieving the best speed-up ratio among all competing methods, while maintaining output consistency with the target model. Underline indicates the best result, while green denotes the second-best result.

LLaVA-1.5		$\mathcal{A} \uparrow$	$\mathcal{R} \uparrow$	LLaVA-1.5		$\mathcal{A} \uparrow$	$\mathcal{R} \uparrow$	FLOPs \downarrow	
Speculative Decoding									
$\tau=0$	Text-only (Gagrani et al., 2024)	0.59	1.42 \times	$\tau=1$	Text-only (Gagrani et al., 2024)	0.52	1.37 \times	70.4T	
	Eagle-MM (Li et al., 2024b)	0.69	1.63 \times		Eagle-MM (Li et al., 2024b)	0.66	1.60 \times	79.5T	
	Medusa-MM (Cai et al., 2024)	2.31	1.69 \times		Medusa-MM (Cai et al., 2024)	2.27	1.63 \times	80.2T	
	SpecVLM (Huang et al., 2025)	0.62	1.46 \times		SpecVLM (Huang et al., 2025)	0.59	1.40 \times	81.0T	
	Dream (Hu et al., 2025)	0.70	1.66 \times		Dream (Hu et al., 2025)	0.68	1.63 \times	79.9T	
	Ours		Ours		VisComp	0.66	1.70 \times	71.2T	
	VisComp	0.68	1.79 \times		SemiAR	2.64	1.76 \times	74.5T	
	SemiAR	2.65	1.77 \times		SpecFLASH	2.63	1.81 \times	70.7T	
	SpecFLASH	2.63	1.83 \times		QwenVL-2.5		QwenVL-2.5		
	Speculative Decoding		Speculative Decoding		$\mathcal{A} \uparrow$	$\mathcal{R} \uparrow$	FLOPs \downarrow		
$\tau=1$	Text-only (Gagrani et al., 2024)	0.70	2.33 \times	$\tau=1$	Text-only (Gagrani et al., 2024)	0.54	1.61 \times	56.3T	
	Eagle-MM (Li et al., 2024b)	0.83	2.49 \times		Eagle-MM (Li et al., 2024b)	0.80	1.93 \times	65.5T	
	Medusa-MM (Cai et al., 2024)	2.76	2.41 \times		Medusa-MM (Cai et al., 2024)	2.65	2.35 \times	67.3T	
	SpecVLM (Huang et al., 2025)	0.64	1.62 \times		SpecVLM (Huang et al., 2025)	0.63	1.58 \times	79.3T	
	Dream (Hu et al., 2025)	0.83	2.51 \times		Dream (Hu et al., 2025)	0.82	2.00 \times	65.7T	
	Ours		Ours		VisComp	0.79	1.99 \times	57.3T	
	VisComp	0.83	2.60 \times		SemiAR	3.09	2.00 \times	61.6T	
	SemiAR	3.28	2.63 \times		SpecFLASH	2.98	2.05 \times	56.8T	
	SpecFLASH	3.21	2.68 \times						

kens as input, and visual instruction tuning, which processes a single image accompanied by textual interactions.

4.2.1. VIDEO CAPTIONING

Table 1 shows the results when using LLaVA-1.5 and QwenVL-2.5 as the target model. τ represents the temperature of the target model, with $\tau = 0$ corresponding to greedy decoding and $\tau = 1$ leading to more diverse outputs. For a fair comparison, the candidate draft length K is fixed at 4 across all speculative decoding models.

In video captioning (VC), the primary challenge lies in effectively processing the visual content while ensuring that the draft model can generate accurate captions. Among the competing models, “Text-only” refers to a speculative decoding method which does not consume visual embeddings and does not generate multimodal-conditioned draft predictions, following the approach proposed by (Gagrani et al., 2024). “Eagle-MM” and “Medusa-MM” refer to variants of Eagle (Li et al., 2024b) and Medusa (Cai et al., 2024), to process image inputs by incorporating a CLIP-style visual encoder and projector, which align visual and textual embeddings into a shared space. These aligned embeddings are concatenated to form the input embeddings and are combined with the second-to-top layer feature F , fol-

lowing the same design as used in the textual components. We observe that although text-only speculative decoding offers some acceleration, its speed-up ratio is inferior to that of multimodal speculative decoding. This is primarily because relying solely on textual context often causes the draft model to generate outputs that diverge from the actual visual content, thereby reducing the overall quality of the generated drafts.

In the LLaVA model, where each image initially consumes 576 tokens, our visual token compression method reduces this to 64 tokens. Comparing previous speculative decoding method “Eagle-MM” and “Medusa-MM” with “VisComp”, we observe that incorporating visual token compression significantly reduces the computational load (FLOPs) and improves the speed-up ratio \mathcal{R} by reducing the number of input tokens, which causes only a minimal decrease in the average acceptance tokens \mathcal{A} . Compared to speculative decoding in the autoregressive setting (“Eagle-MM”), the semi-autoregressive approach (“SemiAR”) demonstrates a significant advantage in terms of average accepted tokens, as it can return multiple draft candidates in a single forward pass. This leads to an overall speed-up ratio improvement of approximately 9.3%. By combining visual token compression with semi-autoregressive inference, SpecFLASH achieves the highest speed-up ratio at about 1.8 \times compared

to the target model.

In the QwenVL model, the number of visual tokens varies with the input image size. To standardize, we resize images to generate 324 tokens per image. Additionally, our visual token compression reduces the token count to 36. Most trends in the QwenVL model align with those observed in LLaVA. Compared to “Eagle-MM”, “VisComp” and “SemiAR” yield additional speed-up gains of approximately 2.6% and 6.3%, respectively. Furthermore, SpecFLASH achieves speed-up ratios of $2.68\times$ and $2.05\times$ over target model under $\tau = 0$ and $\tau = 1$, respectively. These results demonstrate the effectiveness of our method on both LLaVA and QwenVL models.

4.2.2. VISUAL INSTRUCTION TUNING

In visual instruction tuning (VIT), each input consists of an image paired with a textual instruction, covering a broad range of tasks such as image captioning, visual question answering, object recognition, and visual reasoning. Using LLaVA-1.5 and QwenVL-2.5 as the target models, we conduct experiments on VIT task following the same experiment setups as in VC task.

As presented in Table 2, by comparing the “Text-only” with “Eagle-MM” speculative decoding, we find that relying solely on text input leads to a significant drop in the draft generation quality when fine-grained image understanding is required, particularly on LLaVA. Additionally, our proposed visual token compression (“VisComp”) and semi-autoregressive (“SemiAR”) improves the overall speed-up ratio by 2.3% and 7.9%, respectively, comparing to “Eagle-MM”. Specifically, we further find that when temperature $\tau = 0$, using “SemiAR” yields a $0.22\times$ speed-up, which is notably higher than the $0.08\times$ improvement observed at $\tau = 1$. This improvement due to the model’s tendency to produce more deterministic outputs at lower temperatures, which aligns well with the parallel token generation in the semi-autoregressive head.

Notably, “SemiAR” yields greater improvements in VIT than in VC. Besides, we observe that the improvement brought by visual token compression is less pronounced in the visual instruction tuning task compared to VC task. This is likely because visual instruction tuning typically involves a single image, whereas VC tasks process multiple frames. By combining “VisComp” and “SemiAR”, SpecFLASH achieves speed-up ratios of $2.55\times$ and $1.83\times$ on LLaVA and QwenVL, respectively. Moreover, we observe that SpecFLASH efficiently processes visual information while incurring a computational load comparable to that of the “Text-only” model. It enables SpecFLASH to achieve a significantly higher speed-up ratio without sacrificing draft quality. These results further demonstrate the effectiveness of our method across both VC and VIT tasks.

4.2.3. TEXT-ONLY SCENARIO

To further investigate the effectiveness of our method beyond multimodal tasks, we additionally evaluate SpecFLASH in text-only setting. In this case, the visual token compression module becomes inactive, and the draft model operates solely based on the textual prompt.

The results on LLaVA-650k text-only subset are summarized in Table 3. Several observations can be drawn. First, speculative decoding in a text-only setting achieves a $1.63\times$ speed-up, which is lower than that in the multimodal setting. The results indicate that visual input can provide structural cues (e.g., spatial relations) that tend to make generation more predictable. In comparison, text-only sequences generally display more diverse linguistic patterns. Second, SpecFLASH attains $1.88\times$ speed-up in the text-only case ($+0.25\times$ over the text-only baseline), and $2.49\times$ in the multimodal setting ($+0.28\times$ over Eagle-MM).

Overall, these results confirm two key insights: First, visual grounding indeed provides additional structural constraints that amplify the benefits of speculative decoding. Second, SpecFLASH’s semi-autoregressive design and draft architecture remain effective in pure-text scenarios, even though the model is primarily trained on image–text pairs. We hypothesize that explicit exposure to text-only data during training could further boost performance in such cases. These findings highlight the distinct structural properties of multimodal generation and reinforce our claim that semi-autoregressive decoding is particularly well-suited to vision–language models.

4.3. Ablations

To further clarify the contribution of the visual token compression module, we perform an ablation where SpecFLASH is evaluated with different visual compression methods. Results are shown in Table 4.

We observe that our SpecFLASH achieves the best acceleration consistently across both tasks ($2.55\times$ and $1.83\times$). Non-parametric strategies such as average pooling and SGL (Zhao et al., 2025) yield limited speed-up ratio. It suggests that visual token compression module goes beyond simple redundancy-reduction heuristics, providing a more principled design to maximize efficiency. In contrast to previous visual token compression methods like FastV (Chen et al., 2024a) and Twig (Shao et al., 2025), which primarily aim to shorten the input sequence and preserve semantic information, our approach emphasizes inference efficiency. As a result, while their acceleration is limited, it reflects the fact that their design focus was not faster decoding but semantic preservation under compression.

To further explore the trade-off between the draft quality and its efficiency, we vary the scale of the draft model through

Table 2. Quantitative experiments of **visual instruction tuning** on LLaVA-1.5 and QwenVL-2.5. Similar to VC task, we report speed-up ratio \mathcal{R} , average acceptance tokens \mathcal{A} , and average computational cost (FLOPs). SpecFLASH combines “VisComp” and “SemiAR”, achieving the highest speed-up ratio among all competing methods, while maintaining output consistency with the target model. Underline indicates the best result, while green denotes the second-best result.

LLaVA-1.5		$\mathcal{A} \uparrow$	$\mathcal{R} \uparrow$	LLaVA-1.5		$\mathcal{A} \uparrow$	$\mathcal{R} \uparrow$	FLOPs \downarrow	
Speculative Decoding									
$\tau=0$	Text-only (Gagrani et al., 2024)	0.68	1.60 \times	$\tau=1$	Text-only (Gagrani et al., 2024)	0.66	1.52 \times	11.6T	
	Eagle-MM (Li et al., 2024b)	0.76	2.21 \times		Eagle-MM (Li et al., 2024b)	0.76	2.19 \times	12.7T	
	Medusa-MM (Cai et al., 2024)	2.55	2.28 \times		Medusa-MM (Cai et al., 2024)	2.52	2.24 \times	13.0T	
	SpecVLM (Huang et al., 2025)	0.73	1.77 \times		SpecVLM (Huang et al., 2025)	0.69	1.72 \times	13.2T	
	Dream (Hu et al., 2025)	0.72	2.18 \times		Dream (Hu et al., 2025)	0.70	2.14 \times	12.9T	
	Ours		Ours		VisComp	0.76	2.21 \times	11.8T	
	VisComp	0.76	2.23 \times		SemiAR	2.58	2.24 \times	12.0T	
	SemiAR	<u>2.86</u>	2.49 \times		SpecFLASH	<u>2.59</u>	2.29 \times	11.5T	
	SpecFLASH	2.77	2.55 \times	QwenVL-2.5		$\mathcal{A} \uparrow$	$\mathcal{R} \uparrow$	FLOPs \downarrow	
	Speculative Decoding		Speculative Decoding		Text-only (Gagrani et al., 2024)	0.50	1.36 \times	11.4T	
$\tau=0$	Text-only (Gagrani et al., 2024)	0.52	1.44 \times	$\tau=1$	Eagle-MM (Li et al., 2024b)	0.63	1.59 \times	12.6T	
	Eagle-MM (Li et al., 2024b)	0.65	1.63 \times		Medusa-MM (Cai et al., 2024)	2.29	1.65 \times	13.0T	
	Medusa-MM (Cai et al., 2024)	2.36	1.68 \times		SpecVLM (Huang et al., 2025)	0.62	1.50 \times	13.2T	
	SpecVLM (Huang et al., 2025)	0.65	1.52 \times		Dream (Hu et al., 2025)	0.66	1.65 \times	12.7T	
	Dream (Hu et al., 2025)	0.67	1.66 \times	Ours		VisComp	0.60	1.65 \times	
	Ours		Ours		SemiAR	2.38	1.70 \times	11.6T	
	VisComp	0.63	1.69 \times	SpecFLASH	<u>2.46</u>	1.83 \times	11.8T		
	SemiAR	<u>2.46</u>	1.79 \times	SpecFLASH	2.36	<u>1.71</u> \times	11.3T		
	SpecFLASH	<u>2.46</u>	1.83 \times	QwenVL-2.5		$\mathcal{A} \uparrow$	$\mathcal{R} \uparrow$	FLOPs \downarrow	

Table 3. Speed-up ratios under text-only prompts on LLaVA-650k subset.

Method	Image-text pairs	Text-only
Text-only	-	1.63 \times
Eagle-MM	2.21 \times	1.82 \times
SpecFLASH	2.49 \times	1.88 \times

Table 4. Ablation study on different visual token compression methods.

Method	VIT	VC
w/o VisComp	2.49 \times	1.77 \times
Average pooling	2.31 \times	1.77 \times
SGL (Zhao et al., 2025)	1.68 \times	1.80 \times
FastV (Chen et al., 2024a)	1.53 \times	1.60 \times
Twig (Shao et al., 2025)	1.58 \times	1.53 \times
SpecFLASH (ours)	2.55 \times	1.83 \times

adjusting the layer parameters. To be specific, we modify the number of parameters in the draft model, including the number of attention heads and the number of attention layers. The resulting speed-up ratios are reported in Table 5. These results show that balance between the scale of draft model and speed is important. For example, a draft model with 2 Transformer layers may have more accuracy in predicting the target distributions. However, at the same time,

it introduces additional computational cost thus affect the overall speed-up ratios.

Table 5. Speed-up ratios under different draft model scales.

Task	VIT	VC
Head-32/Layer-1 (ours)	2.55 \times	1.83 \times
Head-64/Layer-1	2.56 \times	1.80 \times
Head-16/Layer-1	2.11 \times	1.34 \times
Head-32/Layer-2	1.97 \times	1.55 \times

5. Conclusions

In this work, we introduce SpecFLASH, a novel speculative decoding framework designed specifically for Large Multimodal Models (LMMs). SpecFLASH introduces two key components: a visual token compression module that reduces input redundancy, and a semi-autoregressive decoding strategy that enables parallel token generation. Together, these innovations accelerate multimodal inference while preserving the quality of the output. Experiments on video captioning and visual instruction tuning tasks demonstrate that SpecFLASH delivers substantial speed-ups over existing speculative decoding methods, enabling more efficient deployment of LMMs.

References

Achiam, J., Adler, S., Agarwal, S., Ahmad, L., Akkaya, I., Aleman, F. L., Almeida, D., Altenschmidt, J., Altman, S., Anadkat, S., et al. Gpt-4 technical report. *arXiv preprint arXiv:2303.08774*, 2023.

Bachmann, G., Anagnostidis, S., Pumarola, A., Georgopoulos, M., Sanakoyeu, A., Du, Y., Schönenfeld, E., Thabet, A., and Kohler, J. Judge decoding: Faster speculative sampling requires going beyond model alignment. *arXiv preprint arXiv:2501.19309*, 2025.

Bai, S., Chen, K., Liu, X., Wang, J., Ge, W., Song, S., Dang, K., Wang, P., Wang, S., Tang, J., et al. Qwen2. 5-vl technical report. *arXiv preprint arXiv:2502.13923*, 2025.

Cai, T., Li, Y., Geng, Z., Peng, H., Lee, J. D., Chen, D., and Dao, T. Medusa: Simple llm inference acceleration framework with multiple decoding heads. In *International Conference on Machine Learning*, pp. 5209–5235. PMLR, 2024.

Chen, C., Borgeaud, S., Irving, G., Lespiau, J.-B., Sifre, L., and Jumper, J. Accelerating large language model decoding with speculative sampling. *arXiv preprint arXiv:2302.01318*, 2023.

Chen, L., Zhao, H., Liu, T., Bai, S., Lin, J., Zhou, C., and Chang, B. An image is worth 1/2 tokens after layer 2: Plug-and-play inference acceleration for large vision-language models. In *Proceedings of the European Conference on Computer Vision*, pp. 19–35, 2024a.

Chen, Z., Wu, J., Wang, W., Su, W., Chen, G., Xing, S., Zhong, M., Zhang, Q., Zhu, X., Lu, L., et al. Internvl: Scaling up vision foundation models and aligning for generic visual-linguistic tasks. In *Proceedings of the IEEE/CVF conference on computer vision and pattern recognition*, pp. 24185–24198, 2024b.

Chen, Z., Yang, X., Lin, J., Sun, C., Chang, K., and Huang, J. Cascade speculative drafting for even faster llm inference. *Advances in Neural Information Processing Systems*, 37: 86226–86242, 2024c.

Elhoushi, M., Shrivastava, A., Liskovich, D., Hosmer, B., Wasti, B., Lai, L., Mahmoud, A., Acun, B., Agarwal, S., Roman, A., et al. Layerskip: Enabling early exit inference and self-speculative decoding. In *Proceedings of the 62nd Annual Meeting of the Association for Computational Linguistics (Volume 1: Long Papers)*, pp. 12622–12642, 2024.

Fan, X., Ji, T., Jiang, C., Li, S., Jin, S., Song, S., Wang, J., Hong, B., Chen, L., Zheng, G., et al. Mousi: Polyvisual-expert vision-language models. *arXiv preprint arXiv:2401.17221*, 2024.

Fu, Y., Bailis, P., Stoica, I., and Zhang, H. Break the sequential dependency of llm inference using lookahead decoding. *arXiv preprint arXiv:2402.02057*, 2024.

Gagrani, M., Goel, R., Jeon, W., Park, J., Lee, M., and Lott, C. On speculative decoding for multimodal large language models. In *Proceedings of the IEEE/CVF Conference on Computer Vision and Pattern Recognition*, pp. 8285–8289, 2024.

Ganesan, M., Segal, S., Aggarwal, A., Sinnadurai, N., Lie, S., and Thangarasa, V. Massv: Multimodal adaptation and self-data distillation for speculative decoding of vision-language models. *arXiv preprint arXiv:2505.10526*, 2025.

Gao, X., Xie, W., Xiang, Y., and Ji, F. Falcon: Faster and parallel inference of large language models through enhanced semi-autoregressive drafting and custom-designed decoding tree. In *Proceedings of the AAAI Conference on Artificial Intelligence*, pp. 23933–23941, 2025.

Hu, Y., Xia, T., Liu, Z., Raman, R., Liu, X., Bao, B., Sather, E., Thangarasa, V., and Zhang, S. Q. Dream: Drafting with refined target features and entropy-adaptive cross-attention fusion for multimodal speculative decoding. *arXiv preprint arXiv:2505.19201*, 2025.

Huang, H., Yang, F., Liu, Z., Yin, X., Li, D., Ren, P., and Barssoum, E. Specvilm: Fast speculative decoding in vision-language models. *arXiv preprint arXiv:2509.11815*, 2025.

Kay, W., Carreira, J., Simonyan, K., Zhang, B., Hillier, C., Vijayanarasimhan, S., Viola, F., Green, T., Back, T., Natsev, P., et al. The kinetics human action video dataset. *arXiv preprint arXiv:1705.06950*, 2017.

Leviathan, Y., Kalman, M., and Matias, Y. Fast inference from transformers via speculative decoding. In *International Conference on Machine Learning*, pp. 19274–19286. PMLR, 2023.

Li, J., Li, D., Savarese, S., and Hoi, S. Blip-2: Bootstrapping language-image pre-training with frozen image encoders and large language models. In *International conference on machine learning*, pp. 19730–19742. PMLR, 2023.

Li, W., Yuan, Y., Liu, J., Tang, D., Wang, S., Qin, J., Zhu, J., and Zhang, L. Tokenpacker: Efficient visual projector for multimodal llm. *arXiv preprint arXiv:2407.02392*, 2024a.

Li, Y., Wei, F., Zhang, C., and Zhang, H. Eagle: Speculative sampling requires rethinking feature uncertainty. In *International Conference on Machine Learning*, pp. 28935–28948. PMLR, 2024b.

Li, Y., Wei, F., Zhang, C., and Zhang, H. Eagle-2: Faster inference of language models with dynamic draft trees. In *Proceedings of the 2024 Conference on Empirical Methods in Natural Language Processing*, pp. 7421–7432, 2024c.

Liu, F., Tang, Y., Liu, Z., Ni, Y., Tang, D., Han, K., and Wang, Y. Kangaroo: Lossless self-speculative decoding for accelerating llms via double early exiting. *Advances in Neural Information Processing Systems*, 37:11946–11965, 2024a.

Liu, H., Li, C., Wu, Q., and Lee, Y. J. Visual instruction tuning. *Advances in neural information processing systems*, 36:34892–34916, 2023.

Liu, H., Li, C., Li, Y., and Lee, Y. J. Improved baselines with visual instruction tuning. In *Proceedings of the IEEE/CVF Conference on Computer Vision and Pattern Recognition*, pp. 26296–26306, 2024b.

Liu, R., Gao, J., Zhao, J., Zhang, K., Li, X., Qi, B., Ouyang, W., and Zhou, B. Can 1b llm surpass 405b llm? rethinking compute-optimal test-time scaling. *arXiv preprint arXiv:2502.06703*, 2025.

Muennighoff, N., Yang, Z., Shi, W., Li, X. L., Fei-Fei, L., Hajishirzi, H., Zettlemoyer, L., Liang, P., Candès, E., and Hashimoto, T. s1: Simple test-time scaling. *arXiv preprint arXiv:2501.19393*, 2025.

Shang, Y., Cai, M., Xu, B., Lee, Y. J., and Yan, Y. Llava-prumerge: Adaptive token reduction for efficient large multimodal models. *arXiv preprint arXiv:2403.15388*, 2024.

Shao, Z., Wang, M., Yu, Z., Pan, W., Yang, Y., Wei, T., Zhang, H., Mao, N., Chen, W., and Yu, J. Growing a twig to accelerate large vision-language models. In *Proceedings of the International Conference on Computer Vision*, 2025.

Team, G., Georgiev, P., Lei, V. I., Burnell, R., Bai, L., Gulati, A., Tanzer, G., Vincent, D., Pan, Z., Wang, S., et al. Gemini 1.5: Unlocking multimodal understanding across millions of tokens of context. *arXiv preprint arXiv:2403.05530*, 2024.

Wang, S., Yu, R., Yuan, Z., Yu, C., Gao, F., Wang, Y., and Wong, D. F. Spec-vla: speculative decoding for vision-language-action models with relaxed acceptance. *arXiv preprint arXiv:2507.22424*, 2025.

Wen, Z., Gao, Y., Wang, S., Zhang, J., Zhang, Q., Li, W., He, C., and Zhang, L. Stop looking for important tokens in multimodal language models: Duplication matters more. *arXiv preprint arXiv:2502.11494*, 2025.

Xia, H., Li, Y., Zhang, J., Du, C., and Li, W. Swift: On-the-fly self-speculative decoding for llm inference acceleration. *arXiv preprint arXiv:2410.06916*, 2024a.

Xia, H., Yang, Z., Dong, Q., Wang, P., Li, Y., Ge, T., Liu, T., Li, W., and Sui, Z. Unlocking efficiency in large language model inference: A comprehensive survey of speculative decoding. In *Findings of the Association for Computational Linguistics ACL 2024*, pp. 7655–7671, 2024b.

Yang, A., Yang, B., Zhang, B., Hui, B., Zheng, B., Yu, B., Li, C., Liu, D., Huang, F., Wei, H., et al. Qwen2. 5 technical report. *arXiv preprint arXiv:2412.15115*, 2024.

Yao, L., Li, L., Ren, S., Wang, L., Liu, Y., Sun, X., and Hou, L. Deco: Decoupling token compression from semantic abstraction in multimodal large language models. *arXiv preprint arXiv:2405.20985*, 2024.

Zhang, S., Fang, Q., Yang, Z., and Feng, Y. Llava-mini: Efficient image and video large multimodal models with one vision token. *arXiv preprint arXiv:2501.03895*, 2025.

Zhao, W., Han, Y., Tang, J., Li, Z., Song, Y., Wang, K., Wang, Z., and You, Y. A stitch in time saves nine: Small vlm is a precise guidance for accelerating large vlms. In *Proceedings of the Computer Vision and Pattern Recognition Conference*, pp. 19814–19824, 2025.

Zhou, Y., Lyu, K., Rawat, A. S., Menon, A. K., Ros tamizadeh, A., Kumar, S., Kagy, J.-F., and Agarwal, R. Distillspec: Improving speculative decoding via knowledge distillation. *arXiv preprint arXiv:2310.08461*, 2023.

A. Scale of Draft Model

Other than changing the scale of the draft model by adjusting the number of parameters, we conducted additional experiments by applying quantization to the draft model. The measured speed-up ratios are summarized in Table 6.

Table 6. Quantization on draft model, reporting the speed-up ratio as the primary metric.

Task	VIT	VC
SpecFLASH-fp16	2.55 \times	1.83 \times
SpecFLASH-bf16	2.43 \times	1.79 \times
SpecFLASH-int8	2.44 \times	1.74 \times
SpecFLASH-int4	2.15 \times	1.55 \times

These results show that quantization does not offer the expected further speeding up. We believe this is because our draft model is already lightweight. In such a small model, the efficiency gains from quantization are insufficient to offset the loss in prediction accuracy.

B. Algorithm

Algorithm 1 illustrates the draft generation process. Code is provided in Supplementary Materials.

Algorithm 1 Draft Generation Process

- 1: **Input:** Visual embeddings V , textual embeddings E , number of tokens K , semi-autoregressive head S , compression query \mathcal{C}
- 2: **Output:** Draft tokens T'_1, \dots, T'_K
- 3: // Transformer processing
- 4: $F_V, F_T \leftarrow \text{Transformer.layers}(\text{concat}(V, E))$ {Second-to-top layer visual and textual features}
- 5: // Visual token compression
- 6: $\hat{F}_V \leftarrow \text{softmax}(\mathcal{C}F_V^\top)F_V$ {Compressed visual features}
- 7: // Semi-autoregressive generation
- 8: $\hat{F}_T \leftarrow \text{FC}(\text{concat}(F_T, E_{N+2:M+1}))$ {Textual input features}
- 9: $F' \leftarrow \text{concat}(\hat{F}_V, \hat{F}_T)$ {Concatenate visual and textual inputs}
- 10: $F'_{M+1}, \dots, F'_{M+K} \leftarrow S(F')$ {Semi-autoregressive inference}
- 11: $P'_1, \dots, P'_K \leftarrow \text{LM-head}(F'_{M+1}), \dots, \text{LM-head}(F'_{M+K})$ {Token probability distributions}
- 12: **Return** $T'_1, \dots, T'_K \sim \text{Categorical}(P'_1), \dots, \text{Categorical}(P'_K)$

C. Ablations on Compression Ratios

We further conduct ablations on the scale of \mathcal{C} , which influences the number of visual tokens after compression. The results are presented in Table 7. Our chosen ratio of 1/9 strikes an optimal balance, delivering the peak speed-up. The performance remains robust across a range of ratios (from 1/4 to 1/16), indicating that SpecFLASH is not overly sensitive to the exact compression rate. However, the extreme case of removing visual tokens entirely ($C/N = 0$) leads to a clear performance drop, confirming that our compression module retains essential visual information necessary for maintaining draft quality.

Table 7. Speed-up Ratios with different compression ratios on visual instruct tuning (VIT) and video captioning (VC).

Compression ratios C/N	VIT	VC
1 (w/o compression)	2.49 \times	1.77 \times
1/4	2.51 \times	1.83 \times
1/9 (SpecFLASH)	2.55 \times	1.83 \times
1/16	2.33 \times	1.80 \times
0 (w/o image)	1.92 \times	1.60 \times

D. Ablation on Draft Length K

In traditional speculative decoding, the draft model generates tokens sequentially in an autoregressive manner over K steps. The hyperparameter K is utilized during inference to determine the number of speculative tokens generated per iteration; however, it is not involved in the training phase of the draft model. In contrast, our method employs a semi-autoregressive head to generate K tokens in parallel, making K a critical hyperparameter during both training and inference.

Figure 3 illustrates the impact of different K on the speed-up ratio and average acceptance tokens. When $K = 1$, the draft model generates a single candidate token per forward pass. This model thereby degenerates into an autoregressive speculative decoding. We observe a notable improvement in both the speed-up ratio and average acceptance tokens when increasing K to 4. However, further increasing K to 6 results in only marginal benefits. The average acceptance tokens \mathcal{A} does not increase proportionally with K , suggesting a higher likelihood of token rejection at a larger K .

E. Ablation on Semi-autoregressive Group Size k'

We further conduct ablations on the number of draft tokens produced per forward pass of the draft model k' . For example, when semi-autoregressive group size is $k' = 2$ and the draft length $K = 4$, the draft model first generates 2 draft tokens, then uses these tokens as input to generate the next 2 draft tokens; the resulting 4 draft tokens are subsequently evaluated by the target model. The results in Table 8 show that setting $k' = 4$ yields better speed-up ratios. In this case, the semi-autoregressive head predicts 4 tokens in a single forward pass, and these candidate tokens are then evaluated by the target model.

Table 8. Speed-up ratios with different k' settings.

Method	k'	K	Speed-up ratio
SpecFLASH (main results)	4	4	2.55 \times
SpecFLASH	2	4	2.47 \times
Autoregressive	1	4	2.23 \times

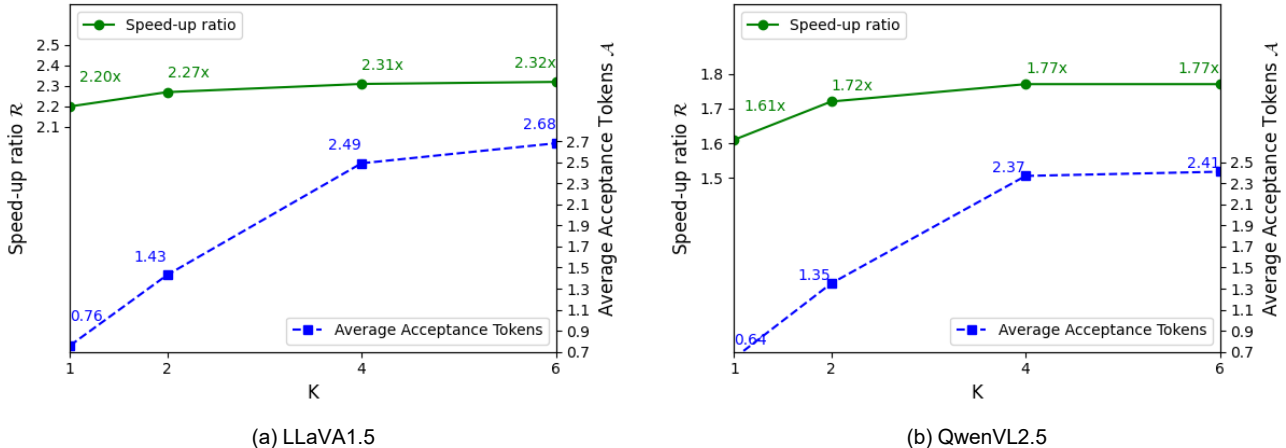


Figure 3. Speed-up ratio and average acceptance tokens with different draft length K . The green solid line indicates the speed-up ratio, while the blue dashed line represents the average acceptance tokens.

Table 9. Quantitative experiments of video captioning, reporting the speed-up ratio as the primary metric.

Model	LLaVA-7B	LLaVA-13B	QwenVL-3B	QwenVL-7B	QwenVL-32B
Eagle-MM	1.63 \times	1.24 \times	2.48 \times	2.49 \times	2.01 \times
SpecFLASH	1.83 \times	1.47 \times	2.65 \times	2.68 \times	2.20 \times

Table 10. Quantitative experiments of visual instruction tuning, reporting the speed-up ratio as the primary metric.

Model	LLaVA-7B	LLaVA-13B	QwenVL-3B	QwenVL-7B	QwenVL-32B
Eagle-MM	2.21 \times	1.21 \times	1.88 \times	1.63 \times	1.40 \times
SpecFLASH	2.55 \times	1.49 \times	2.01 \times	1.83 \times	1.49 \times

F. Scalability

To validate the robustness of our approach, we further conducted experiments using LLaVA-13B, QwenVL-3B, QwenVL-32B, in addition to the main results reported on LLaVA-7B and QwenVL-7B. The results in Table 9 and Table 10 show that SpecFLASH consistently achieves a higher speed-up ratio compared to multimodal speculative decoding, a variant of Eagle adapted to handle multimodal input (Eagle-MM). This highlights the efficiency of SpecFLASH in both video captioning and instruction tuning tasks.

G. Multi-Task Evaluation of Visual Instruction Tuning

Visual instruction tuning encompasses multiple tasks, such as fine-grained image captioning, ScienceQA, and commonsense reasoning. We evaluate the performance on each benchmark individually. The results demonstrate that SpecFLASH consistently outperforms the competing methods across all tasks, indicating its robustness.

Table 11. Performance comparison on multiple tasks.

Method	COCO Captioning	MMT-Bench	ScienceQA
EAGLE-MM	2.28 \times	2.26 \times	2.15 \times
DREAM	2.49 \times	2.23 \times	2.11 \times
SpecFLASH	2.64 \times	2.38 \times	2.32 \times

H. Limitations and Future works

Experiments demonstrate that SpecFLASH consistently accelerates both video captioning and visual instruction tuning. Importantly, SpecFLASH has the potential to serve as a general-purpose acceleration method on a wide range of multimodal tasks, as visual instruction tuning itself encompasses multiple such tasks. We intend to extend our approach to additional multimodal tasks in future work. Furthermore, the semi-autoregressive decoding strategy can experience reduced acceptance rates as the draft length increases. Although these trade-offs did not significantly impact the results reported here, they indicate that further investigation into adaptive compression techniques and more flexible decoding strategies will be important for achieving broader and more reliable deployment.